WFS1-Associated Optic Neuropathy : Genotype-Phenotype Correlations and Disease Progression

Majander, Anna

2022-09

Majander , A , Jurkute , N , Burte , F , Brock , K , Joao , C , Huang , H , Neveu , M M , Chan , C M , Duncan , H J , Kelly , S , Burkitt-Wright , E , Khoyratty , F , Lai , Y T , Subash , M , Chinnery , P F , Bitner-Glindzicz , M , Arno , G , Webster , A R , Moore , A T , Michaelides , M , Stockman , A , Robson , A G & Yu-Wai-Man , P 2022 , ' WFS1-Associated Optic Neuropathy : Genotype-Phenotype Correlations and Disease Progression ' , American Journal of Ophthalmology , vol. 241 , pp. 9-27 . https://doi.org/10.1016/j.ajo.2022.04.003

http://hdl.handle.net/10138/346328
https://doi.org/10.1016/j.ajo.2022.04.003

WFS1-Associated Optic Neuropathy: Genotype-Phenotype Correlations and Disease Progression

ANNA MAJANDER, NERINGA JURKUTE, FLORENCE BURTÉ, KRISTIAN BROCK, CATARINA JOÃO, HOUBIN HUANG, MAGELLA M. NEVEU, CHOI MUN CHAN, HOLLY J. DUNCAN, SIMON KELLY, EMMA BURKITT-WRIGHT, FADIL KHOYRATTY, YOON TSE LAI, MALA SUBASH, PATRICK F. CHINNERY, MARIA BITNER-GLINDZICZ, GAVIN ARNO, ANDREW R. WEBSTER, ANTHONY T. MOORE, MICHEL MICHAELIDES, ANDREW STOCKMAN, ANTHONY G. ROBSON, AND PATRICK YU-WAI-MAN

• OBJECTIVE: To evaluate the pattern of vision loss and genotype-phenotype correlations in *WFS1*-associated optic neuropathy (WON).
• DESIGN: Multicenter cohort study.
• METHODS: The study involved 37 patients with WON carrying pathogenic or candidate pathogenic *WFS1* variants. Genetic and clinical data were retrieved from the medical records. Thirteen patients underwent additional comprehensive ophthalmologic assessment. Deep phenotyping involved visual electrophysiology and advanced psychophysical testing with a complementary metabolomic study.
Main Outcome Measures: *WFS1* variants, functional and structural optic nerve and retinal parameters, and metabolomic profile.
• RESULTS: Twenty-two recessive and 5 dominant *WFS1* variants were identified. Four variants were novel. All *WFS1* variants caused loss of macular retinal ganglion cells (RGCs) as assessed by optical coherence tomography (OCT) and visual electrophysiology. Advanced psychophysical testing indicated involvement of the major RGC subpopulations. Modeling of vision loss showed an accelerated rate of deterioration with increasing age. Dominant *WFS1* variants were associated with abnormal reflectivity of the outer plexiform layer (OPL) on OCT imaging. The dominant variants tended to cause less severe vision loss compared with recessive *WFS1* variants, which resulted in more variable phenotypes ranging from isolated WON to severe multisystem disease depending on the *WFS1* alleles. The metabolomic profile included markers seen in other neurodegenerative diseases and type 1 diabetes mellitus.
• CONCLUSIONS: *WFS1* variants result in heterogenous phenotypes influenced by the mode of inheritance and the disease-causing alleles. Biallelic *WFS1* variants cause more variable, but generally more severe, vision and RGC loss compared with heterozygous variants. Abnormal cleftlike lamination of the OPL is a distinctive OCT feature that strongly points toward dominant WON. (Am J Ophthalmol 2022;241: 9–27. © 2022 The Author(s). Published by Elsevier Inc. This is an open access article under the CC BY license (http://creativecommons.org/licenses/by/4.0/))

AJO.com Supplemental Material available at AJO.com.
Accepted for publication April 13, 2022.

From the UCL Institute of Ophthalmology (A.M., N.J., C.J., M.M.N., C.M.C., M.S., G.A., A.R.W., A.T.M., M.M., A.S., A.G.R., P.Y.-W.-M.), London, United Kingdom; Moorfields Eye Hospital (A.M., N.J., M.M.N., C.M.C., G.A., A.R.W., A.T.M., M.M., A.G.R., P.Y.-W.-M.), London, United Kingdom; Department of Ophthalmology, Helsinki University Hospital, University of Helsinki (A.M.), Helsinki, Finland; Biosciences Institute, International Centre for Life, Newcastle University (F.B.), Newcastle upon Tyne, United Kingdom; Cancer Research UK Clinical Trials Unit, University of Birmingham (K.B.), Birmingham, United Kingdom; Hainan Hospital of the General Hospital of Chinese People's Liberation Army (H.H.), Sanya, China; Newcastle Eye Centre, Royal Victoria Infirmary (H.J.D.), Newcastle upon Tyne, United Kingdom; Bolton NHS Foundation Trust (S.K., F.K., Y.T.L.), Bolton, United Kingdom; Manchester Centre for Genomic Medicine, Manchester University NHS Foundation Trust (E.B.-W.), Manchester, United Kingdom; Division of Evolution and Genomic Sciences, University of Manchester, Manchester Academic Health Sciences Centre (E.B.-W.), Manchester, United Kingdom; MRC Mitochondrial Biology Unit, Department of Clinical Neurosciences, University of Cambridge (P.F.C.), Cambridge, United Kingdom; Great Ormond Street Hospital, Great Ormond Street, London (M.B.-G.), United Kingdom; Department of Ophthalmology, UCSF School of Medicine (A.T.M.), San Francisco, California, USA; John van Geest Centre for Brain Repair and MRC Mitochondrial Biology Unit, Department of Clinical Neurosciences, University of Cambridge (P.Y.-W.-M.), Cambridge, United Kingdom; and Cambridge Eye Unit, Addenbrooke's Hospital, Cambridge University Hospitals (P.Y.-W.-M.), Cambridge, United Kingdom

Inquiries to Anna Majander, Department of Ophthalmology, Helsinki University Hospital, Helsinki, Finland.; e-mail: anna.majander@hus.fi

The WFS1 gene encodes for a transmembrane protein, wolframin, which localizes to the endoplasmic reticulum (ER).[1] Wolframin is highly expressed in the human retina, including Müller and retinal ganglion cells (RGCs).[2] Optic neuropathy is one of the major diagnostic criteria for Wolfram syndrome type 1 caused by biallelic pathogenic variants in *WFS1* (4p16.1, OMIM 606201).[3,4] Wolfram syndrome type 1 is a severe, progressive neurodegenerative multisystem disorder that was originally described by its defining features of diabetes insipidus, diabetes mellitus, optic atrophy, and deafness

0002-9394/$36.00
https://doi.org/10.1016/j.ajo.2022.04.003

(DIDMOAD).[3] However, expanding genetic testing has revealed that pathogenic *WFS1* variants can result in a much more diverse range of phenotypes, which can be less severe with some heterozygous variants having a dominant mode of inheritance.[5,6]

Optic neuropathy associates with homozygous or compound heterozygous *WFS1* variants, referring to an autosomal recessive (AR) disease, and with only 1 pathogenic *WFS1* allele, referring to an autosomal dominant (AD) disease. However, only a relatively small subgroup of the >200 reported pathogenic *WFS1* variants cause dominant disease.[4-7] *WFS1*-associated optic neuropathy (WON) is usually diagnosed in childhood and there is progressive loss of RGCs with thinning of the retinal nerve fiber layer (RNFL).[8-12] It has been suggested that the severity of the ocular phenotype correlates with the burden of neurologic complications and with the inheritance pattern.[13] More recently, some patients have been reported with a milder nonsyndromic AR disease limited to optic atrophy or in combination with hearing loss.[13] Because of the relative rarity of WON and its variable genotype, there are limited data on its natural history and the factors that modulate disease progression.

Here, we report a comprehensive ophthalmologic assessment of WON, as part of an ongoing deep-phenotyping study of patients with inherited optic neuropathies.[14,15] Our aims were to characterize genotype-phenotype correlations and the pattern and progression of visual impairment in WON. A subgroup of the *WFS1* patient cohort was characterized with complementary ophthalmologic, electrophysiological, and psychophysical investigations. In addition to the phenotypic data, the level of circulatory metabolite markers was determined in serum samples of patients with WON and compared with *OPA1*-associated dominant optic atrophy (*OPA1* DOA) and healthy controls.

PATIENTS AND METHODS

• **PATIENT ENROLLMENT AND GENETIC ANALYSIS:** The study had ethical and institutional approval (Moorfields Eye Hospital NHS Foundation Trust, London; the Newcastle Eye Centre, Royal Victoria Infirmary, Newcastle upon Tyne; the Royal Bolton Hospital, Bolton), and its design complied with the Declaration of Helsinki. The multicenter study cohort of 37 patients with a diagnosis of inherited optic neuropathy and *WFS1* variants was ascertained in the Genetic Service at Moorfields Eye Hospital NHS Foundation Trust (London, UK), the Newcastle Eye Centre, Royal Victoria Infirmary (Newcastle upon Tyne, UK), and Bolton NHS Foundation Trust (Bolton, Greater Manchester, UK). *WFS1* genetic testing was conducted in accredited molecular genetic laboratories.

External databases (Genome Aggregation Database [gnomAd, https://gnomad.broadinstitute.org], ClinVar [https://www.ncbi.nlm.nih.gov/clinvar], and LOVD [*Leiden Open Variation Database*, https://www.lovd.nl]) and prediction algorithms (Polymorphism Phenotyping version 2 [PolyPhen-2, http://genetics.bwh.harvard.edu/pph2] and Mutation Taster [http://www.mutationtaster.org]) were used to assess *WFS1* variant frequency and pathogenicity. ACMG (American College of Medical Genetics) classification for each variant is also provided.[16]

For the purpose of comparative analyses, data from patients with DOA and disease-causing variants in *OPA1* gene were included as detailed in the advanced psychophysics and metabolomic sections.

• **CLINICAL ASSESSMENT:** Clinical data of the diagnostic and follow-up examinations of 37 patients were retrieved by retrospective review of the medical records from the different study sites. Thirteen of these patients were examined as part of the NIHR RD-TRC Inherited Optic Neuropathy study at Moorfields Eye Hospital NHS Foundation Trust (London, UK). Three of them underwent advanced psychophysical investigations. Blood samples were collected from 9 patients for metabolomic analysis.

The following demographic and clinical data were recorded: *WFS1* genotype, detailed family history, sex, age at diagnosis of WON, extraocular abnormalities, best-corrected visual acuity (BCVA), visual field, red-green color discrimination using Ishihara pseudoisochromatic plates, optical coherence tomography (OCT) imaging of optic disc and macula, and visual electrophysiology. Visual fields were studied using either automated Humphrey visual field perimetry (Humphrey Visual Field Analyzer, Model 750; Humphrey Instruments) or Goldmann perimetry. The assessment profile for each patient in relation to the imaging, visual field, psychophysical, electrophysiological, and metabolomic analyses is indicated in Table 1.

BCVA was recorded using either the Early Treatment Diabetic Retinopathy Study (ETDRS) or Snellen charts. The Snellen fractions were converted to logMAR units. For 2 elderly patients (P5, P7), no visual acuity data were available. Therefore, BCVA data of 35 patients, 18 of whom had AR and 17 AD WON, were included in the study. Follow-up BCVA data were available for 33 patients, 18 with AR and 15 with AD disease, with BCVA measurements obtained for at least 2 time points. The visual acuity values potentially affected by ocular diseases other than WON, or of the level of light perception, were not included in the analysis. Mean and median BCVA for the AR and AD subgroups were calculated using the first available BCVA value for each patient.

Altogether, 246 BCVA values were used for the longitudinal analysis. Hierarchical regression models were used to estimate longitudinal BCVA outcomes. Population-level effects, also known as fixed effects, were included to reflect the average response seen across all patients at all times

TABLE 1. Demographic, Genetic, and Clinical Data of the WON Study Group

Patient	Sex	Inheritance (Family)GC Number	Genotype: *WFS1* Variant	Age at Diagnosis of WON, y	Other Clinical Features	Macular OCT FindingsOPL Cleft / INL Cysts+ or -[Age (y)[a]]	Complementary Tests
1	F	AD (D1) 17594	c.2051C>T: p.Ala684Val	5	HI, epilepsy, hypertension [b]	+/– [46]	VF, E, ME
2	M	AD (D1) 17594	c.2051C>T: p.Ala684Val	23	HI	+/– [23]	VF, E
3	M	AD (D1) 17594	c.2051C>T: p.Ala684Val	13	HI	np	E
4	F	AD (D1) 17594	c.2051C>T: p.Ala684Val	3	HI	+/+ [3]	E
5	M	AD (D1) 17594	c.2051C>T: p.Ala684Val	U	HI	np	
6	F	AD (D2)	c.2051C>T: p.Ala684Val	60	HI [b]	+/– [78]	VF
7	M	AD (D3)	c.2051C>T: p.Ala684Val	U	HI, DM1	np	VF
8	F	AD (D4)	c.2051C>T: p.Ala684Val	38	HI	+/+ [71]	VF
9	F	AD (D4)	c.2051C>T: p.Ala684Val	28	HI	+/– [48]	VF
10	F	AD (D4)	c.2051C>T: p.Ala684Val	6	HI	+/+ [24]	VF
11	M	AD (D4)	c.2051C>T: p.Ala684Val	4	HI	+/+ [18]	VF
12	M	AD (D5) 25494	c.2051C>T: p.Ala684Val	16	HI	+/– [18]	VF, E
13	F	AD (D6) 22818	c.2051C>T: p.Ala684Val	40	aHI, DM2, DM related peripheral neuropathy [b]	+/+ [64]	
14	F	AD (D7) 15095	c.2390A>T: p.Asp797Val	45	HI, DM2 [b]	+/+ [69]	E
15	F	AD (D8) 17496	c.968A>G: p.His323Arg	30	HI	+/+ [44]	VF, E
16	F	AD (D8) 17496	c.968A>G: p.His323Arg	4	HI	+/+ [8]	VF, E
17	F	AD (D9)	c.2161A>T: p.Asn721Tyr	50	HI, nystagmus	+/+ [51]	ME
18	M	AD (D9)	c.2161A>T: p.Asn721Tyr	U	HI	np	ME
19	M	AD de novo (D10) 22794	c.937C>T: p.His313Tyr	7	HI, DM1, short stature, learning disability	+/– [10]	VF, E
20	F	AR (R1)	c.1234_1237delCTGT; p.Val412Serfs*29 c.1673G>A; p.Arg558His	5	DM1, NB	np	VF
21	F	AR (R2)	c.409_424dup16; p.Val142Glyfs*110 c.2194C>T; p.Arg732Cys	U	DM2	np	VF, ME
22	F	AR (R3) 17712	c.2648_2651delTCTT p.Phe883Serfs*68 c.2213C>A; p.Ala738Asp	10	None	–/– [31]	

(*continued on next page*)

TABLE 1. (*continued*)

Patient	Sex	Inheritance (Family)GC Number	Genotype: *WFS1* Variant	Age at Diagnosis of WON, y	Other Clinical Features	Macular OCT FindingsOPL Cleft / INL Cysts+ or -[Age (y)[a]]	Complementary Tests
23	M	AR (R3) 17712	c.2648_2651delTCTT p.Phe883Serfs*68 c.2213C>A; p.Ala738Asp	10	Polyuria	–/– [26]	
24	F	AR (R4) 17782/22809	c.2648_2651delTCTT: p.Phe883Serfs*68 c.1597C>T: p.Pro533Ser	23	DI, NB, BI	–/– [44]	VF, E, P
25	F	AR (R4) 22809	c.2648_2651delTCTT: p.Phe883Serfs*68 c.1597C>T: p.Pro533Ser	37	DI, NB, BI	–/– [52]	VF, E, P
26	F	AR (R5) 26525	c.2648_2651delTCTT p.Phe883Serfs*68 c.505G>A: p.Glu169Lys	10	HI, DM1, NB	–/– [15]	VF
27	M	AR (R6)	c.1558C>T; p.Gln520* c.1372G>A;p.Ala458Thr	24	DM1	np	VF, ME
28	F	AR (R7)	c.1309G>C;p.Gly437Arg c.977C>T; p.Ala326Val	18	DM1	np	ME
29	F	AR (R8)	c.1549delC; P.Arg517Alafs*5 c.1597C>T; p.Pro533Ser[c]	17	HI, NB	np	
30	M	AR (R9)	c.2648_2651delTCTT p.Phe883Serfs*68 c.1433G>A; p.Trp478*	12	DM1, DI, NB	np	VF, P, ME
31	F	AR (R10)	c.409_424dup16: p.Val142Glyfs*110 c.2262_2263delCT: p.Cys755Serfs*3	31	HI, DM1	–/– [35]	ME
32	M	AR (R11) 20579	c.874C>A: p.Pro292Thr c.505G>A: p.Glu169Lys	9	DM1, DI, HI, NB, BI	–/– [45]	
33	M	AR (R11) 20579	c.874C>A: p.Pro292Thr c.505G>A: p.Glu169Lys	U	DM1, DI, HI, NB, BI	–/– [46]	VF
34	F	AR (R12) 17240	c.2643_2644delC:p.Phe883Leufs*56 (homozygous)	15	HI, DM1, DI, bipolar affective disorder [b]	–/– [25]	
35	M	AR (R13) 25698	c.1232_1233celCT: p.Ser411Cysfs*131 (homozygous)	8	HI, DM1	–/– [10]	VF
36	M	AR (R14) 24848	c.1243_1245del, p.Val415del c.1885C>T, p.Arg629Trp	4	HI, DM1	np	

(*continued on next page*)

TABLE 1. (*continued*)

Patient	Sex	Inheritance (Family)GC Number	Genotype: *WFS1* Variant	Age at Diagnosis of WON, y	Other Clinical Features	Macular OCT FindingsOPL Cleft / INL Cysts+ or -[Age (y)[a]]	Complementary Tests
37	F	AR (R15) 22817	c.1283C>G; p.Pro428Arg c.2319C>G; p.Tyr773*	10	DM1, UC, ataxia, depression	–/– [23]	VF, ME

AD = autosomal dominant, aHI = acquired hearing impairment due to measles encephalitis at the age of 6 years, AR = autosomal recessive, DI = diabetes insipidus, DM1 = diabetes mellitus type 1, DM2 = diabetes mellitus type 2, E = visual electrophysiology, HI = hearing impairment, ME = metabolomics, NB = neurogenic bladder, np = not performed, OCT, optic coherence tomography, OPL = outer plexiform layer, P = psychophysics, RNFL = peripapillary retinal nerve fiber layer, U = Unknown, UC = urinary and faecal incontinence, VF = visual field; WON = *WFS1*-associated optic neuropathy.

The GC number refers to our genetics database coding system.

[a]Age when macular SD-OCT was performed.

[b]Additional clinical features were as follows—Patient P1: myopia; patient P6: cataract at the age of 77 years; patient P13: high myopia, bilateral posterior cataracts and left epiretinal membrane; patient P14: cataract at the age of 63 years and left epiretinal membrane; patient P34: intermittent myoclonus, occasional balance problem, postural hypotension.

[c]Also a carrier of the *GJB2* pathogenic variant c.35delG p.(Gly12Valfs*2).

(the intercept), separate gradients with respect to time in the AR and AD patient groups, and further nonlinear functions of time, as required. Group-level effects, also known as random effects, were used at the patient and eye levels to reflect that outcomes for an eye are correlated through time and that eyes for a patient are also highly correlated.

• **OCT IMAGING:** High-resolution spectral-domain optical coherence tomography (SD-OCT) data were acquired with the Spectralis (Heidelberg Engineering Ltd) and Cirrus HD-OCT 4000 (Carl Zeiss Meditec, Inc) platforms. For peripapillary RNFL measurements, a 3.5-mm-diameter circular scan centered on the optic disc was used and the sectorial data were collected and compared to the normative data. Automated segmentation and thickness analyses of 10 retinal layers were performed for perifoveal volumetric retinal B-scans using the Heidelberg Engineering segmentation tool, included in the Spectralis Glaucoma Module software (version 6.0), as previously described.[15,17] Normative data were generated from SD-OCT images of 48 healthy eyes of 48 subjects.[17]

• **VISUAL ELECTROPHYSIOLOGY:** Twelve patients underwent visual electrophysiological testing according to the standard protocols of the International Society for Clinical Electrophysiology of Vision (ISCEV).[18,19] The tests included the pattern reversal visual evoked potential (PVEP), flash visual evoked potential (FVEP), and pattern electroretinogram (PERG). Pattern ERGs were recorded to a 0.8° check size using both a standard checkerboard field (12 × 15°) and additionally to a large field (24 × 30°).[20] International-standard full-field ERGs were recorded using gold foil corneal electrodes in 9 patients. In addition to standard measurements, the photopic negative response (PhNR) component of the light-adapted single flash (LA 3) ERG was assessed.[21] Two amplitude ratios, N95-P50 of PERG and PhNR–b-wave of the LA 3 ERG, were additionally computed, with the PhNR amplitude measured from the preceding b-wave peak to PhNR trough.[15] The results were compared to reference normative data.

• **ADVANCED PSYCHOPHYSICAL INVESTIGATIONS:** Three patients (P24, P25, and P30) underwent advanced psychophysical investigations using previously described methodology.[14] The normal subjects for psychophysical tests were 15 individuals aged 17-78 years at the time of testing with normal BCVA and normal color vision as assessed by standard color vision tests. Data for 9 patients with *OPA1* DOA were used for comparative analyses, and their details have previously been reported (patients P3, P4, P6, P9, P10, P11, P17, P18, and P23).[14]

The test conditions for the following tests were as previously described by the same investigators.[14,15] Achromatic spatial contrast sensitivity was measured as a function of spatial frequency. The target stimuli were horizontally orientated Gabor patterns with spatial frequencies ranging from 0.5 to 16 cycles per degree (cpd) and with a spatial Gaussian window with a standard deviation of 6°.[14] Chromatic discrimination was tested using the so-called trivector test procedure implemented as part of the Cambridge Colour Test, version 1.5 (Cambridge Research Systems Ltd).

The test conditions included the modification for observers with reduced visual acuity and the viewing distance of 62.6 cm so that the Landolt "C" opening subtended 5° of visual angle.[14] L-cone temporal acuities (critical flicker fusion, cff) were measured using a Maxwellian-view opti-

cal system. The L-cone stimulus was produced by flickering a 650-nm circular target of 4° visual angle in diameter superimposed in the center of a steady 481-nm circular background field of 9° diameter.[14,15,22,23]

• **STATISTICAL ANALYSIS:** Independent samples Mann-Whitney *U* was used for comparison of distribution of continuous variables in the various patient subgroups and controls. Spearman rank correlation were used for the analysis of statistical dependence between various variables as indicated in the Results section. The SPSS, version 25 (IBM Corp), and R, version 3.6 (The R Foundation for Statistical Computing), were used for the analyses.

• **METABOLOMIC ANALYSIS:** For the metabolomic analysis, blood samples were collected from 9 WON patients, 9 gender-matched *OPA1* DOA patients, and 9 gender-matched healthy individuals as healthy controls (HC). The WON group (patients P1, P17, P18, P21, P27, P28, P30, P31, and P37) included 6 patients with AR and 3 patients with AD WON (Table 1). Ages between WON patients, *OPA1* DOA patients, and healthy controls were matched with means ± standard error of the mean (SEM) of 42 ± 4 years for both *WFS1* and HC groups, and 44 ± 4 years for the *OPA1* DOA group.

Serum samples were immediately processed after collection, aliquoted, and maintained at –80°C until required. As part of a wider metabolomic study, these samples were randomized among other patient cohorts with inherited optic neuropathies and assigned a unique identifier, prior to being sent to Metabolon Inc for processing. Proteins were precipitated with methanol under vigorous shaking for 2 minutes (Glen Mills GenoGrinder 2000) followed by centrifugation. The resulting extract was divided into 5 fractions: 2 for analysis by 2 separate reverse-phase (RP) / ultraperformance liquid chromatography (UPLC)–tandem mass spectrometry (MS/MS) methods with positive ion mode electrospray ionization (ESI), 1 for analysis by RP/UPLC-MS/MS with negative ion mode ESI, 1 for analysis by HILIC/UPLC-MS/MS with negative ion mode ESI, and 1 sample was reserved for backup.

Samples were placed briefly on a TurboVap (Zymark) to remove the organic solvent. All samples were processed on an UPLC and Q-Exactive high resolution/accurate mass spectrometer (Thermo Scientific) interfaced with a heated electrospray ionization (HESI-II) source and Orbitrap mass analyzer operated at 35,000 mass resolution. The MS analysis alternated between MS and data-dependent MSn scans using dynamic exclusion. The scan range varied slighted between methods but covered 70-1000 *m/z*. Raw data were extracted, peak-identified, and QC processed using Metabolon's hardware and software. Identification of known chemical entities was based on comparison to metabolomic library entries of purified standards. Using this protocol, 1319 metabolites were detected and 1018 metabolites were positively identified

MetaboAnalyst, version 4.0,[24] and R, version 3.6 (The R foundation for Statistical Computing), were used in combination for data preprocessing, statistical analysis, and visualization of univariate and multivariate analyses. Metabolites that were present in less than 25% of all samples were filtered out. Blank data for the remaining metabolites were imputed as half of the minimum positive value. Data was then standardized using *z* scores. The number of metabolites detected in the final analysis was 694, with 585 metabolites being positively identified. Statistical significance when comparing WON, *OPA1* DOA and HC groups was evaluated by 1-way analysis of variance with Benjamini-Hochberg correction for multiple hypothesis testing (FDR values), followed by Fisher least significant difference post hoc test for pairwise comparisons.

RESULTS

• ***WFS1* GENOTYPE:** The study cohort included 37 patients (22 females and 15 males) with WON. Their demographic, genetic, and clinical data are presented in Table 1. The results of the assessment of the pathogenicity using external databases and the ACMG classification are presented for each variant in Table 2. Nineteen patients from 10 families carried a single heterozygous pathogenic *WFS1* variant compatible with AD WON (Table 1). All dominant variants were missense.

Patients P17 and P18 (a mother and her son) carried a novel rare heterozygous *WFS1* variant c.2161A>T (p.Asn721Tyr), which has not been reported in the gnomAD database. This variant affects a conserved amino acid and based on in silico analysis it was predicted to be disease-causing (Table 2) and was not detected in 3 unaffected family members. In addition, variants c.2390A>T (p.Asp797Val) and c.968A>G (p.His323Arg) were identified for the first time in the single heterozygous state in patients with optic neuropathy (P14, P15, and P16).

Eighteen patients from 15 families carried 22 different variants in the compound heterozygous or homozygous state in keeping with an AR pattern of inheritance. Eleven of these *WFS1* variants led to either a frame-shift or an early stop codon, and 11 were missense variants. Three patients (P1, P2, and P22) carried compound heterozygous missense variants, whereas in 10 patients only 1 of the alleles was missense. Two homozygous variants leading to an early stop codon were identified in 2 patients with one of the variants, c.2643_2644delC (p.Phe883Leufs*56), being previously unreported. In addition, 1 probably damaging, c.1372G>A (p.Ala458Thr), and 1 likely benign, c.2213C>A (p.Ala738Asp), missense variants were novel (Table 2). All 3 patients carrying these novel missense variants had a previously reported pathogenic *WFS1* variant as the second allele.

TABLE 2. *WFS1* Gene Variants in the Study Population

Genotype, *WFS1* Variant	Patients(n)	Exon	Allele Frequency gnomAD(all)	Prediction PolyPhen2(score)	Prediction Mutation Taster	ClinVar Interpretation (No. of Submissions)	LOVD	ACMG Classification	First Published Report*
AD inheritance									
c.2051C>T, p.Ala684Val	13	8	VNF	Probably damaging (1.0)	Disease causing	Pathogenic (8)	Pathogenic	Pathogenic: PS3, PM1, PM2, PP2, PP3, PP5	Tessa et al[49]
c.2390A>T, p.Asp797Val	1	8	VNF	Possibly damaging (0.826)	Disease causing	—	—	Likely pathogenic: PM2, PM5, PP2, PP3	Rohayem et al[40]; patient reported in Majander et al[17]; not reported in AD disease in other cohorts
c.968A>G, p.His323Arg	2	8	VNF	Probably damaging (0.997)	Disease causing	—	—	Likely pathogenic: PM2, PP1, PP2, PP3, PP5,	Smith et al[44]; patients reported in Majander et al[17]; not reported in AD disease in other cohorts
c.2161A>T, p.Asn721Tyr	2	8	VNF	Possibly damaging (0.826)	Disease causing	—	—	Likely pathogenic: PM2, PP1, PP2, PP3	Patients reported in Majander et al[17]; not reported in other cohorts
De novo									
c.937C>T, p.His313Tyr	1	8	VNF	Probably damaging (0.974)	Disease causing	Likely pathogenic (1)	—	Likely pathogenic: PS2, PM2, PP2, PP3, PP5	Hansen et al[42]
AR inheritance									
c.505G>A, p.Glu169Lys	2	5	0.00002483	Probably damaging (1.0)	Disease causing	Uncertain significance (1)	—	Likely pathogenic: PM2, PM5, PP1, PP2, PP3	Hardy et al[46]
c.874C>A, p.Pro292Thr		8	0.000007966	Probably damaging (1.0)	Disease causing	—	—	Likely pathogenic: PM2, PP1, PP2, PP3, PP5	Astuti et al[50]
c.2648_2651delTCTT, p.Phe883Serfs*68	2	8	0.00009239	—	Disease causing	Pathogenic (2) Likely pathogenic (1)	—	Pathogenic: PVS1, PM2, PP1, PP3, PP5	Hardy et al[46]
c.1597C>T, p.Pro533Ser		8	0.0007487	Probably damaging (1.0)	Disease causing	Benign (1) Likely benign (1) Uncertain significance (3)	VUS	Likely pathogenic: PM1, PM2, PM5, PP1, PP2, PM3, PP3	Crawford et al[51]; patients reported in Majander et al[17]; not reported in optic neuropathy or Wolfram syndrome in other cohorts
c.2643_2644delC, p.Phe883Leufs*56 (homozygous)	1	8	VNF	—	Disease causing	—	—	Pathogenic: PVS1, PM2, PP3, PP5	Patient reported in Majander et al[17]; not reported in other cohorts
c.409_424dup16, p.Val142Glyfs*110	1	4	0.00004386	—	Disease causing	Pathogenic (3)	—	Pathogenic: PVS1, PM2, PP5	Rohayem et al[40]

(*continued on next page*)

TABLE 2. (*continued*)

Genotype, *WFS1* Variant	Patients(n)	Exon	Allele Frequency gnomAD(all)	Prediction PolyPhen2(score)	Prediction Mutation Taster	ClinVar Interpretation (No. of Submissions)	LOVD	ACMG Classification	First Published Report*
c.2262_2263delCT, p.Cys755Serfs*3		8	VNF	—	Disease causing	—	—	Pathogenic: PVS1, PM2, PP3	Khanim et al[7]
c.1232_1233delCT, p.Ser411Cysfs*131 (homozygous)	1	8	0.000003977	—	Disease causing	—	—	Pathogenic: PVS1, PM2, PP3	Giuliano et al[48]
c.1433G>A, p.Trp478*	1	8	0.00002003	—	Disease causing	—	—	Pathogenic: PVS1, PM2, PP3	Hardy et al[46]
c.2648_2651delTCTT, p.Phe883Serfs*68		8	0.00009239	—	Disease causing	Pathogenic (2) Likely pathogenic (1)	—	Pathogenic: PVS1, PM2, PP3, PP5	Hardy et al[46]
c.1558C>T, p.Gln520*	1	8	0.000003991	—	Disease causing	—	—	Pathogenic: PVS1, PM2, PP3	Giuliano et al[48]
c.1372G>A, p.Ala458Thr		8	0.00003188	Probably damaging (0.990)	Disease causing	—	—	VUS: PM2, PM3, PP3	Not reported
c.1283C>G, p.Pro428Arg	1	8	VNF	Probably damaging (1.0)	Disease causing	—	—	Likely pathogenic: PM1, PM2, PP3, BP1, PM3	Astuti et al[50]
c.2319C>G, p.Tyr773*		8	VNF	—	Disease causing	—	—	Pathogenic: PVS1, PM2, PP3	Astuti et al[50]
c.1549delC, P.Arg517fs*5	1	8	VNF	—	Disease causing	—	—	Likely pathogenic: PVS1, PM2	Hardy et al[46]
c.1597C>T, p.Pro533Ser		8	0.0007487	Probably damaging (1.0)	Disease causing	Benign (1) Likely benign (1) Uncertain significance (2)	VUS	VUS: PM2, PP3, BP1	Crawford et al[51]; not reported in optic neuropathy or Wolfram syndrome in other cohorts
c.1309G>C, p.Gly437Arg	1	8	0.000003983	Benign (0.029)	Polymorphism	—	—	Likely benign: PM2, PP5	Hardy et al[46]
c.977C>T, p.Ala326Val		8	0.00004951	Probably damaging (0.997)	Disease causing	Uncertain significance (1)	—	Likely benign: PM2, PP3, BP1, BP6	Toppings et al[52]
c.409_424dup16, p.Val142Glyfs*110	1	4	0.00004386	—	Disease causing	Pathogenic (3)	—	Pathogenic: PVS1, PM2, PP5	Gómez-Zaera et al[53]
c.2194C>T, p.Arg732Cys		8	0.00006092	Probably damaging (1.0)	Disease causing	Uncertain significance (1)	VUS	VUS: PM2, PM3, PP3	La Morgia et al[54]
c.1234_1237delCTGT, p.Val412Serfs*29	1	8	0.000003976	—	Disease causing	—	—	Likely pathogenic: PVS1, PM2	Gasparin et al[55]

(*continued on next page*)

TABLE 2. (*continued*)

Genotype, *WFS1* Variant	Patients(n)	Exon	Allele Frequency gnomAD(all)	Prediction PolyPhen2(score)	Prediction Mutation Taster	ClinVar Interpretation (No. of Submissions)	LOVD	ACMG Classification	First Published Report*
c.1673G>A, p.Arg558His		8	0.00006383	Probably damaging (1.0)	Disease causing	Likely pathogenic (1)	—	Likely pathogenic: PM2, PM5, PP3, PP5	Smith et al[44]
c.2213C>A, p.Ala738Asp	2	8	0.00005054	Benign (0.011)	Disease causing	—	—	Likely pathogenic: PM2, PM3, PP1	Not reported
c.2648_2651delTCTT, p.Phe883Serfs*68		8	0.00009239	—	Disease causing	Pathogenic (2) Likely pathogenic (1)	—	Pathogenic: PVS1, PM2, PP5	Hardy et al[46]
c.1243_1245del, p.Val415del	1	8	0.00004772	—	Disease causing	Pathogenic (2)	—	Likely pathogenic: PM1, PM2, PM4, PP3, PP5	Hardy et al[46]
c.1885C>T, p.Arg629Trp		8	0.00001195	Probably damaging (0.996)	Polymorphism	—	—	VUS: PM2, PP5	Giuliano et al[48]
c.505G>A, p.Glu169Lys	1	5	0.00002483	Probably damaging (1.0)	Disease causing	Uncertain significance (1)	—	Likely pathogenic: PM2, PM3, PP3, PP5	Hardy et al[46]
c.2648_2651delTCTT, p.Phe883Serfs*68		8	0.00009239	—	Disease causing	Pathogenic (2) Likely pathogenic (1)	—	Pathogenic: PVS1, PM2, PP3, PP5	Hardy et al[46]

AD = autosomal dominant, VNF = variant not found, VUS = variant of uncertain significance.

Novel variants have been highlighted in bold.

*First report of the *WFS1* variant in an individual with Wolfram syndrome, optic neuropathy or other clinical manifestation.As of this writing, 862 single-gene variants have been reported on ClinVar database (accessed March 19, 2022).Variants' pathogenicity are annotated based on ACMG guidelines using Varsome (accessed May 28, 2021).Databases and sources: Genome Aggregation Database, gnomAd, https://gnomad.broadinstitute.org; Polymorphism Phenotyping version 2, PolyPhen-2, http://genetics.bwh.harvard.edu/pph2; Mutation Taster, http://www.mutationtaster.org; ClinVar, https://www.ncbi.nlm.nih.gov/clinvar; LOVD, Leiden Open Variation Database, https://www.lovd.nl); ACMG, American College of Medical Genetics.[16]

All dominant and homozygous recessive *WFS1* variants, and at least 1 of the alleles of the compound heterozygous variants were located in exon 8. The dominant variants affected either the first transmembrane helix or the endoplasmic ER domain of the wolframin protein (Supplemental Figure S1).

• **EXTRAOCULAR MANIFESTATIONS:** All patients, except 1 patient with AR WON (P22), had extraocular abnormalities, including hearing impairment in 27 patients (73%); type 1 diabetes mellitus in 14 patients (38%); type 2 diabetes mellitus in 3 patients (8%); a neurogenic bladder, urinary or bowel incontinence in 10 patients (27%); diabetes insipidus in 6 patients (16%); and neurologic or psychiatric problems in 5 patients (14%) (Table 1). The pattern of extraocular manifestations was influenced by the *WFS1* variant subtype. All 19 patients with AD WON had hearing deficits, although in 1 patient this was thought to be due to measles encephalitis. Four of the 19 patients with AD WON had diabetes mellitus. Thirteen of the 18 patients (72%) with AR WON had diabetes mellitus, 10 (56%) had urinary or bowel dysfunction, and 8 (44%) had hearing deficits.

• **OPTIC NEUROPATHY:** WON was diagnosed at a median age of 15 years (range = 3-60 years). The median age was 11 years in the AR WON subgroup (range = 4-37 years) and 23 years in the AD WON subgroup (range = 3-60 years). This difference was not statistically significant ($P = .358$).

The peripapillary RNFL thickness data was available for 55 eyes of 28 patients, and the thickness was reduced by 50% compared with normal (SD = 15%) (Supplemental Figure S2). The decrease in RNFL thickness was most prominent in the temporal (mean ± SD = 45% ± 14 %) and inferior (mean ± SD = 44% ± 8%) quadrants, with the temporal quadrant being the most severely affected in 28 eyes and the inferior quadrant in 18 eyes. The severity and the sectoral distribution of RNFL loss were similar ($P > .1$) in patients with AR and AD WON.

At the time of optic disc imaging, there was no statistically significant difference in age between patients with AR WON (n = 17, median age = 33 years, range = 10-51 years) and those with AD WON (n = 11, median age = 22 years, range = 6-72 years, $P = .853$). Regression analysis did not show any significant reduction in RNFL thickness over the age range of the patients in any of the 4 quadrants (data not shown). Sequential RNFL assessments, which were available for 9 patients (4 with AR and 5 with AD WON), did not indicate progressive RNFL loss during a median follow-up period of 2.8 years. The 2 youngest patients (aged 6 and 7 years) who harbored AD WON had similar RNFL loss (mean reduction of 49% compared with normal, SD = 12%).

Three elderly patients (P6, P13, and P14) with severe AD WON had other ocular conditions, namely, cataract, high myopia, or an epiretinal membrane (Table 1). One patient (P17) had nystagmus.

• **MACULAR SD-OCT FINDINGS:** Twenty-six patients underwent macular SD-OCT imaging, including 14 patients (P1, P2, P6, P14-17, P19, P24-25, and P31-34) from the previously published study.[17] In all 15 patients with AD WON (detailed in Table 1), the outer plexiform layer (OPL) had an abnormal, bilateral, symmetrical reflectivity composed of 3 distinct laminae: an innermost highly reflective lamina, a middle nonreflective lamina, and an outermost highly reflective lamina (Figure 1). This feature was not observed in any of the 11 patients with AR WON. In 2 eyes of 2 patients (P13 and P14) with AD WON, a longstanding epiretinal membrane confounded precise OPL evaluation. Nine patients with AD WON also presented with microcystic inner nuclear layer (INL) changes, which was not observed in any of the eyes of patients with AR WON.

Thickness analysis of individual retinal layers in the macula was performed in 40 eyes of 21 patients (Table 3). In addition to the RNFL, the ganglion cell layer–inner plexiform cell layer (GCL-IPL) complex was significantly thinner (mean reduction of 49% compared with normal, SD = 8%) in the *WFS1* group, with the thinning being more severe in eyes with AR compared with AD WON ($P < .001$). The INL thickness was significantly increased (thicker than + 1 SD level of the normal) in 8 of the 16 eyes with AD WON and in 1 of the 24 eyes with AR WON. INL microcystic or microcystoid changes were observed in 9 patients (Table 1).

The eyes with AD WON and abnormal OPL lamination had thicker OPL and combined OPL and outer nuclear layer (ONL) complex compared with normal eyes ($P < .001$), or the eyes with AR WON and normal OPL lamination ($P < .001$). Similar to peripapillary RNFL thickness, regression analysis did not show any significant reduction in thickness for the individual retinal layers over the age range of the WON patients. Sequential macular SD-OCT imaging, which was available for 16 patients with a mean follow-up time of 2.8 years, also did not show any progressive thinning (data not shown).

• **BEST-CORRECTED VISUAL ACUITY AND VISUAL FIELDS:** The median BCVA was 0.78 logMAR (mean ± SD = 1.0 ± 0.60 logMAR) in the AR WON and 0.30 logMAR (mean ± SD = 0.59 ± 0.62 logMAR) in the AD WON subgroup ($P < .001$). There was no significant difference in age between these 2 groups ($P = .829$), with a median age of 29 years in the AR group (mean ± SD = 31 ± 13 years) and 28 years in the AD group (mean ± SD = 34 ± 24 years). However, vision loss varied more in patients with AR WON (shown in order of increasing severity of vision loss in Table 1). Cross-sectional and longitudinal analyses revealed an age-associated worsening of BCVA in patients older than 8 years (Figure 2, A). We first investigated simple models for BCVA deterioration that were linear in time,

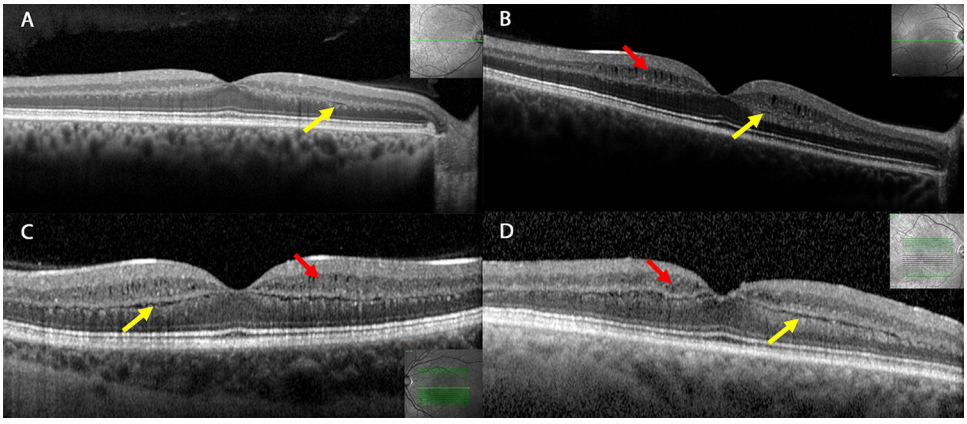

FIGURE 1. Macular spectral-domain optical coherence tomography (SD-OCT) images of patients with autosomal dominant *WFS1*-associated optic neuropathy. SD-OCT images of (A) patient P9, (B) P11, (C) P10, and (D) P8 show characteristic outer plexiform layer lamination (OPL) defects. The yellow arrows indicate the cleft-like middle structure of the OPL. The red arrows highlight areas of microcystoid edema within the inner nuclear layer. (For interpretation of the references to colour in this figure legend, the reader is referred to the web version of this article.)

TABLE 3. Mean Thickness of the Retinal Layers in Eyes of Patients With WON

Retinal Layer	Thickness, μm (Mean ± SD)				
	AR WON (n=24)	P^a	AD WON (n=16)	P^b	Controls (n=48)
Retina	287.1± 11.6	<.001* <.001*	323.0 ± 14.0	<.001*	340.8 ± 13.3
RNFL	17.6 ± 2.3	<.001* .025*	21.0 ± 5.7	.001*	24.2 ± 2.1
GCL-IPL	42.1 ± 4.5	<.001* <.001*	51.1 ± 7.3	<.001*	93.5 ± 7.8
INL	43.5 ± 3.5	.002* .001*	51.2 ± 8.9	<.001*	39.6 ± 3.5
OPL	30.1 ± 2.9	.090 <.001*	51.8 ± 13.0	<.001*	32.3 ± 4.0
OPL-ONL	104.4 ± 8.6	.176 <.001*	117.2 ± 9.0	<.001*	102.0 ± 8.6
Outer retina	79.6 ± 3.1	.026* .126	81.4 ± 2.7	.932	81.5 ± 2.7

AD = autosomal dominant, AR = autosomal recessive, GCL-IPL = ganglion cell–inner plexiform layer, INL = inner nuclear layer, OPL = outer plexiform layer, OPL-ONL = outer plexiform–outer nuclear layer complex, RNFL = retinal nerve fiber layer; WON = *WFS1*-associated optic neuropathy.

[a]Independent samples Mann-Whitney *U* test for the comparisons between AR WON eyes and control eyes (the upper *P* value), and between AR and AD WON eyes (the lower value).

[b]Independent samples Mann-Whitney *U* test for the comparison between AD WON eyes and control eyes.

*Statistically significant *P* value.

that is, the rate of progression for an eye was assumed to be constant over time. When the rate of progression within a patient was allowed to vary with age, it became apparent that the deterioration in BCVA accelerated over time, that is, the gradients were higher for older patients as demonstrated by best fits (lines) for individual eyes (Figure 2, A).

This observation justified the use of nonlinear transformations of time in the model. Models that estimated progression as a quadratic function of time were found to be a good fit (Figure 2,A). The expected group-level progression is shown as bold lines and the model-fitted eye-specific series as faint lines. At all ages, the expected BCVA in patients with AR WON was worse compared with patients with AD WON. Furthermore, the estimated rate of progression was higher in the AR subgroup although the progression rates are expected to converge as time progresses.

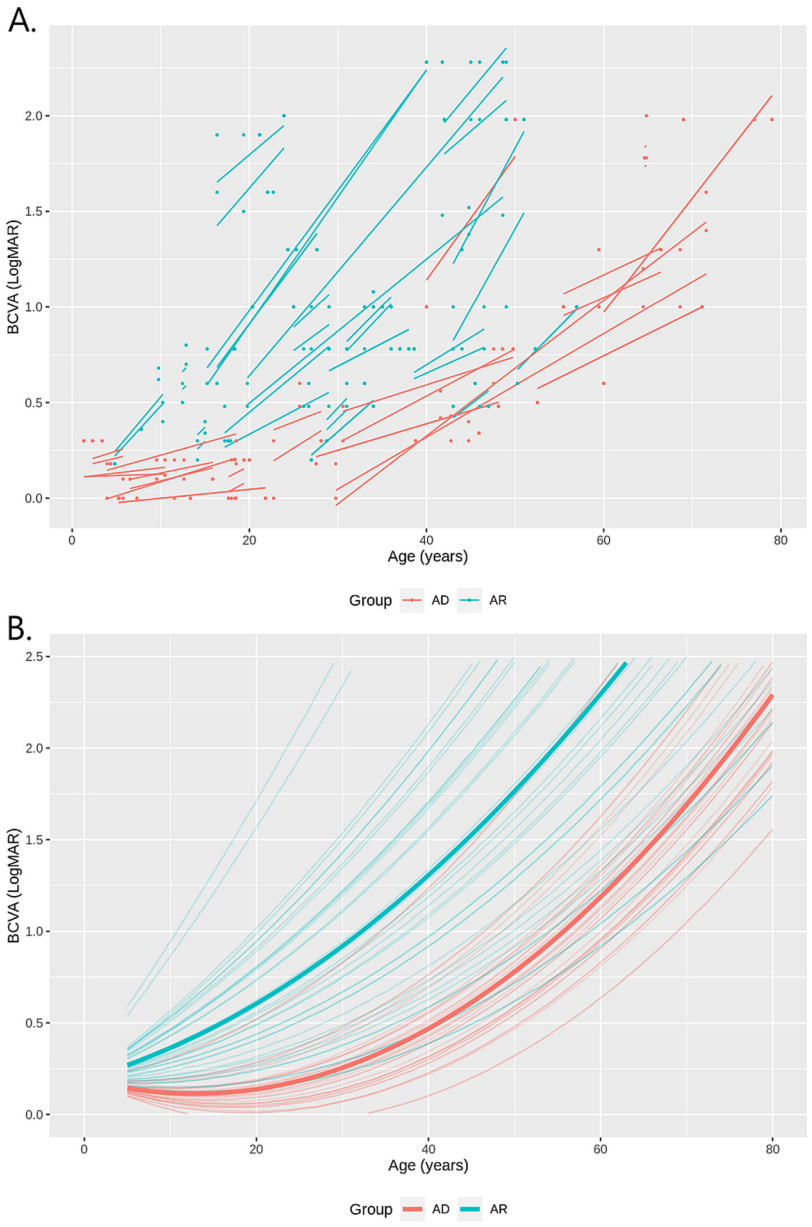

FIGURE 2. Best-corrected visual acuity (BCVA). A. BCVA data from 70 eyes of 18 patients with autosomal recessive (AR) and 17 patients with dominant (AD) *WFS1*-associated optic neuropathy have been plotted as a function of patient age. The lines represent longitudinal assessments for each eye. B. Estimated BCVA progression as a quadratic function of time. The expected group-level progression (AR and AD) are shown as bold lines and the model-fitted eye-specific series as faint lines.

For instance, the expected annual progression is approximately 3.5 times faster in the AR subgroup at age 20 years, 2.2 times faster at age 30 years, and 1.6 times faster at age 40 years compared with the AD subgroup.

Sequential follow-up data of 5 children aged <8 years showed normal developmental maturation of BCVA despite marked peripapillary RNFL and macular GCL-IPL losses. Humphrey visual field data (30-2 or 24-2) was available for 11 and Goldmann static perimetry for 5 patients. The following patterns of visual field loss were observed (Supplemental Figure S3): (1) enlargement of the blind spot; (2) perifoveal sensitivity loss in the superior central field; (3) perifoveal sensitivity loss in the inferior central field; and (4) dense scotomas in the central field leaving only midperipheral field remnants.

• **VISUAL ELECTROPHYSIOLOGY:** Twelve patients underwent visual electrophysiological testing (Figure 3, Supple-

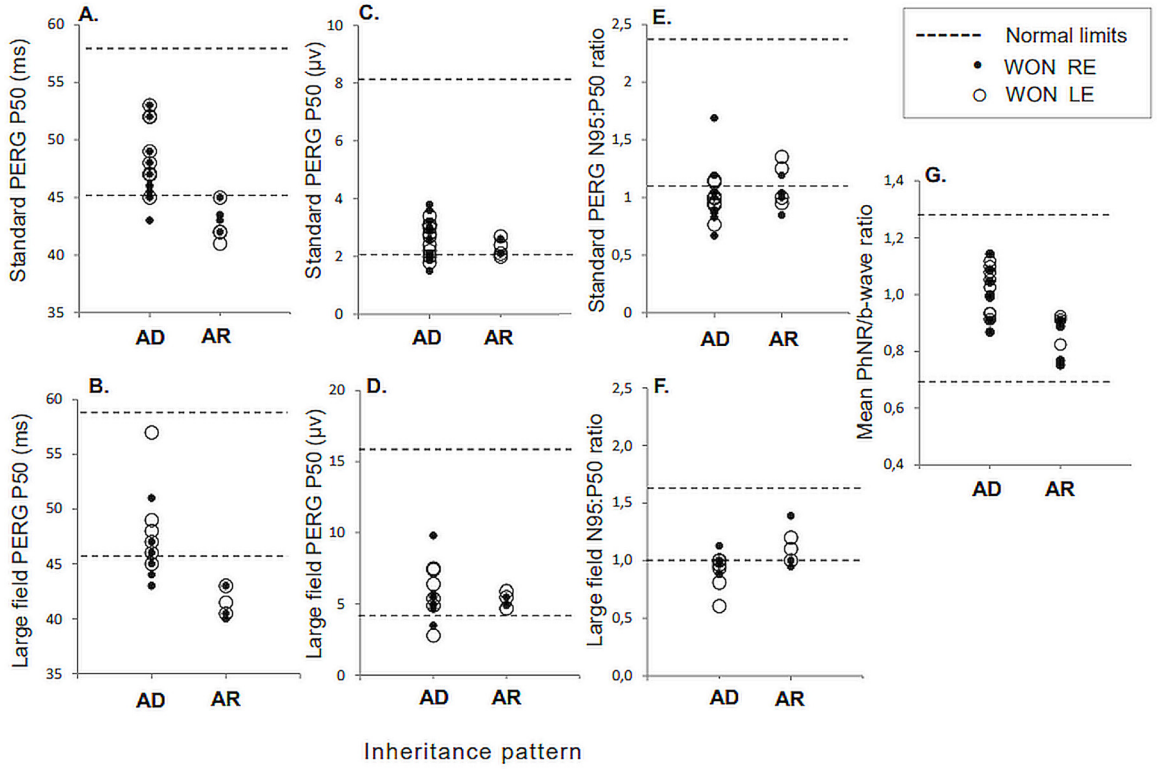

FIGURE 3. Pattern electroretinograms. Standard and large field pattern electroretinograms (PERG) P50 peak time (A, B), amplitude (C, D), and PERG N95-P50 ratio (E, F) for patients with optic neuropathy and autosomal dominant (AD) and autosomal recessive (AR) *WFS1* variants. Mean PhNR/b-wave ratio (G) for 6 patients with AD and 4 patients with AR disease.

mental Figure S4). Four patients had AR WON (age range at the time of testing = 8-50 years) and 8 patients had AD WON (age range at the time of testing = 7-57 years). Only 2 patients had normal PVEPs, whereas the rest had either delayed or undetectable (2 eyes) responses (Supplemental Figure S4, B and C). Delayed VEPs showed additional amplitude reduction (<4 µV) in 5 eyes.

FVEPs were within normal limits in 17 eyes, whereas 5 eyes had subnormal amplitude (<5 µV), of which 2 had delayed FVEP peak time (P2 > 140 ms) (Supplemental Figure S4, D and E). PVEP and FVEP amplitudes showed regression with age (Spearman rho –0.665, $P = .001$, and –0.565, $P = .006$, respectively). PVEPs were similar in the AR and AD WON eyes, but the FVEP peak time was delayed only in the AD WON eyes ($P = .005$). In addition to altered VEP amplitudes and latencies, VEP waveforms were abnormal in patients with AR WON but not with AD WON (Supplemental Figure S4, A).

On PERG testing, normal or borderline N95-P50 amplitude ratios for the standard (Figure 3, E) and large stimulus fields (Figure 3, F) were detected in 6 of the 26 and 9 of the 18 studied eyes, respectively. In contrast, the PERG P50 amplitude was within normal limits in all except 2 eyes (Figure 3, C and D). The PERG P50 peak time was normal (≥45.5 ms) in only 2 of the 8 studied AR WON eyes (Figure 3, A and B). In comparison, peak time was normal in all except 1 of the 18 and 4 of 12 studied AD WON eyes for the standard and large stimulus fields, respectively (Figure 3, A and B).

International-standard full-field ERGs did not reveal any a- or b-wave abnormalities in the 9 WON patients who underwent testing. The PhNR component from the LA 3 ERG responses and the PhNR/b-wave ratios were calculated from 18 eyes of 9 patients. The PhNR/b-wave ratios were within the normal range in all AR and AD cases, although most AD WON cases showed a higher ratio than for the AR cases (Figure 3, G).

• **ADVANCED PSYCHOPHYSICS:** Three AR WON patients (P24, P25, and P30) underwent advanced psychophysical tests. Their results were compared to normative data and to those obtained for 9 age (median = 43 years, range = 19-55 years) and visual acuity (BCVA range = 0.7-1.1 logMAR) matched patients with *OPA1* DOA. Peripapillary RNFL thickness of the 3 patients with AR WON was 50% of normal and thinner compared with the *OPA1* DOA patient group (63% of normal, $P = .036$). In contrast, the macular GCL-IPL complex was thinner in the *OPA1* DOA eyes

(mean ± SD = 37.6 ± 5.9 μm) than in the AR WON eyes (mean ± SD = 44.9 ± 1.6 μm) ($P = .019$).

The WON patients had severely reduced achromatic spatial contrast sensitivity function (SCSF) in all spatial frequencies (colored triangles in Supplemental Figure S5, A). The sensitivity losses for WON patients compared with normal observers (gray triangles in Supplemental Figure S5, A) ranged from between 4 and 30 times at 0.5 cpd and increased with frequency (colored circles, Supplemental Figure S5, A). Moreover, their SCSFs had abnormal low-pass shape with no discernible intermediate peak in sensitivity, observed at 2 cpd for the normal observers. In comparison, the *OPA1* DOA patients exhibited less abnormal and severely reduced SCSF (red inverted triangles and circles; Supplemental Figure S5, A).

In the Cambridge Colour Test, patient P25 was able to detect the protan and deutan targets only at the maximal color saturation of the test (1600×10^{-4} $u'v'$ units [the CIE 1976 $u'v'$ color space]), and the tritan target at approximately 50% saturation (785×10^{-4} $u'v'$ units [the CIE 1976 $u'v'$ color space]), whereas patients P24 and P30 were unable to detect even the most saturated colors. Red-green color discrimination was severely abnormal or unrecordable also in 8 of the 9 WON patients who underwent Ishihara test. In contrast, all *OPA1* DOA patients included in this study were capable of color perception, although with impaired sensitivities and mean vector lengths of 534, 589, and 1012×10^{-4} $u'v'$ units (the CIE 1976 $u'v'$ color space) in the protan, deutan, and tritan confusion lines, respectively (normal values: protan = 45 ± 15; deutan = 43 ± 12; and tritan = $52 \pm 19 \times 10^{-4}$ $u'v'$ units).

In all 3 AR WON patients, L-cone temporal acuity (cff) was severely abnormal (colored circles in Supplemental Figure S5, B) as compared to the normal observers (gray triangles in Supplemental Figure S5, B and C). Flicker was first detected at mean radiances between 7.2 and 8.2 $\log_{10}$ quanta s^{-1} deg^{-2} and cff did not begin to rise until about 8.5 $\log_{10}$ quanta s^{-1} deg^{-2}, which is almost 100 times more intense than that for the normal observers, and 10 times more intense than for the *OPA1* DOA patients (red triangles in in Supplemental Figure S5, C).

The upper bound of flicker rate was reduced ranging from 20 to 26 Hz in the WON patients as compared to 40 Hz of the normal observers. Increases in cff for all observers, including patients with WON and *OPA1* DOA, showed a nearly linear dependence of the cff on the logarithm of target radiance, a property that is known as obedience to the Ferry-Porter law (blue lines in Supplemental Figure S5, C). In the WON and *OPA1* DOA patients, the Ferry-Porter slopes were similar, but shallower compared with the slope for normal observers.

• **METABOLOMICS:** For the metabolomic study, a total of 27 patients were evaluated comprising 9 patients with WON, 9 with *OPA1* DOA, and 9 healthy controls (HCs). Following quality data analysis, 585 metabolites with positive identity were included in the analysis. Multivariate analysis using principal components analysis showed high overlap in variance between the 3 groups, with the first component mildly separating the patients with WON—which constituted the most heterogenous group—from the other 2 groups (Figure 4, A).

In addition, unsupervised orthogonal partial least squares discriminant analysis discriminated well between patients with WON and healthy controls ($Q^2 = 0.673$, $R^2 = 0.896$, $P < .001$), indicating differences driven by the 2 group's respective metabolomes. Using multiple testing, up to 16 metabolites were statistically different in the WON group compared with the HC group (FDR < 0.05; Figure 4, B), with 7 metabolites being also differentially expressed in the *OPA1* DOA group (Supplemental Table S1). Glucose levels were specifically increased in patients with WON but not, or only mildly increased in those with *OPA1* DOA (Figure 4, C).

A similar trend was observed with fatty acid metabolites including acyl carnitines and long-chain fatty acids (Supplemental Table S1). Other metabolites linked to dipeptides, xenobiotics, and nucleotide metabolisms were increased in both the WON and *OPA1* DOA groups (eg, histidylglutamate; Figure 4, D). Lysophospholipids with a structural role (membrane components) were also dysregulated in these 2 patient groups compared with the HC group (eg, 1-docosahexaenoyl-GPC; Figure 4, E).

Cluster analysis of the 16 significantly modulated metabolites showed a distinct clustering of HC compared with the WON and *OPA1* DOA groups. Within the WON group, 5 patients who had type 1 diabetes mellitus (P27, P28, P30, P31, and P37) clustered separately from the patients with *OPA1* DOA. The remaining 4 patients in the WON group who did not have type 1 diabetes mellitus (P1, P17, P18, and P21) overlapped with the patients with *OPA1* DOA (Figure 4, B). This dual clustering within the WON patient group emphasizes the strong metabolomic signature in serum from type 1 diabetes mellitus compared with the metabolomic signature from a more localized degenerative process affecting the optic nerve.

• **DISCUSSION:** This study included 37 patients with optic neuropathy associated with 27 *WFS1* gene variants, 4 of which are novel. Dominant WON was identified in half of the patients, comprising a third of the families studied, and the phenotype in this group was characterized by a combination of optic atrophy and hearing loss. In comparison, AR WON resulted in a far more heterogenous clinical presentation, ranging from the severe, multisystemic Wolfram syndrome, to variable combinations of neurologic and endocrinologic deficits, and isolated optic atrophy.

A unique feature seen in all patients with AD WON, including the patient with the de novo c.937C>T (p.His313Tyr) variant, was the striking OCT signs of abnormal cleft-like lamination and thickening of the OPL, which we have previously described.[17] In addition, patients

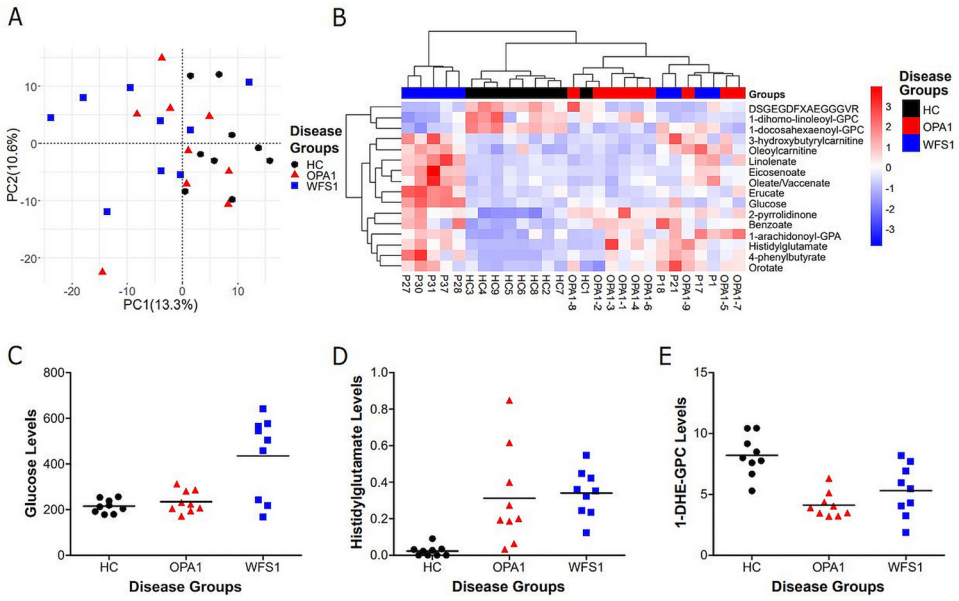

FIGURE 4. Metabolomic profile in patients with *WFS1*-associated optic neuropathy (WFS1) and *OPA1*-associated dominant optic atrophy (OPA1). A. Principal components analysis showing covariance between the 3 groups: WFS1, OPA1 and healthy controls (HC). B. Heatmap representing Euclidian hierarchical cluster analysis including the 16 significant metabolites across the 3 groups using a 1-way analysis of variance with a Benjamini-Hochberg correction for multiple hypothesis testing (FDR < 0.05). C-E. Dot plots representing mean ± SEM for representative metabolites present in heatmap, namely, (C) glucose, (D) histidylglutamate, and (E) 1-docohexaenoyl-glycerophosphatidylcholine (1DHE-GPC).

with AD disease had microcystoid changes or thickening of the INL. Such a microcystic or cystoid-like INL edema is a nonspecific feature seen in both inherited and acquired optic neuropathies,[25] whereas the cleftlike OPL reflectivity appears to be virtually pathognomonic for AD WON.[17]

Based on the known spatial relationships between the OPL sublayers, the presence of bending and radiating Müller cells in the interphase between the inner OPL and Henle fiber layer, and the putative optical fiber–like characteristics of Müller cells, we proposed that the OPL abnormalities on OCT imaging could be due to light being reflected differently by hypertrophic bending Müller cells.[17,26-29] Müller cell swelling and dysfunction also has been proposed as a source for the microcystic or cystoid-like INL edema.[26,30] A common pathophysiological mechanism linked to Müller cells could, therefore, provide a unifying hypothesis for the concurrence of the OPL and INL changes in patients with AD WON. The reasons why AD *WFS1* variants result in selective OPL and INL changes readily visible on OCT imaging require further investigation, in particular, the potential role of Müller cells in driving the underlying pathophysiology.

The visual outcome was strongly influenced by the nature of the *WFS1* allele(s) and the pattern of inheritance. All AD *WFS1* variants were associated with relatively slow visual deterioration, whereas in AR WON, the rate of visual loss was variable, but generally faster. Irrespective of a recessive or dominant mode of inheritance, visual loss in *WFS1* disease is progressive and our modeling indicates that the rate of deterioration accelerates over time.

Consistent with the visual acuity data, the visual electrophysiological abnormalities indicated more severe RGC dysfunction in patients with AR WON than in those with AD WON. Unlike the few published reports describing retinopathy changes as late-stage manifestations of WON, the full-field ERG showed no evidence of generalized photoreceptor or bipolar cell dysfunction in either AR WON (with abnormally thin retinal outer layers) or AD WON (with the characteristic OPL lamination).[3,31,32] RGC dysfunction is, therefore, likely to be the sole contributor to visual deterioration in *WFS1* spectrum disease.

To our knowledge, our study is the first to report on PERG and PhNR findings in patients with WON showing abnormal PERG, but normal full-field PhNR–b-wave ratios, which suggests preferential involvement of macular RGCs.[3,31,33,34] Consistent with a severe loss of the most abundant midget parvocellular RGCs in the macula, most tested patients had poor red-green color vision and all 3 patients with AR WON who underwent psychophysical testing had impaired spatial contrast sensitivity.

However, they also had reduced temporal visual acuity, needing brighter light for motion perception, and they showed absent tritan (S-cone mediated) color vision, indicating additional losses of the less abundant magnocellu-

lar parasol and bistratified koniocellular RGCs.[14,15] Overall, WON was associated with more extensive and severe impairment of visual perception compared with *OPA1* DOA with similar BCVA and degree of macular RGC loss.

Metabolomic profile of our patients with WON reflected their endocrinologic and neurodegenerative manifestations. Metabolites dysregulated in patients with type 1 diabetes mellitus (hexose glucose, acyl carnitines and long-chain fatty acids) were also increased in diabetic WON patients.[35] A similar metabolomic profile has been reported in a *wfs1* knockout mouse model.[36] Metabolomic profile shared by the WON and *OPA1* DOA study groups, namely, low levels of glycerophosphatidylcholines accompanied by high levels of glycerophosphatidic acids, was recently reported in Parkinson disease.[37]

Decreased levels of phosphatidylcholines, lysophosphatidylcholines, and sphinganines have previously been found in patients with Wolfram syndrome, but not in patients with type 1 diabetes mellitus, suggesting that these could be biomarkers of optic nerve degeneration.[38] A decrease in lysophosphocholine levels is suggestive of plasma membrane destabilization and dysregulation of the cell signaling pathways controlling Ca^{2+} homoeostasis, cellular proliferation, survival, migration, and adhesion as a result of G-protein–coupled receptor modulation, all of which have been implicated in the pathophysiology of Wolfram syndrome.[39] A more detailed assessment of the metabolomic profile in *WFS1* spectrum disease will require a larger patient cohort, which is challenging, given that it is an ultrarare disorder.

Exon 8 of the *WFS1* gene was affected in all studied patients. All dominant and homozygous recessive variants, and at least 1 of the compound heterozygous recessive variants, were located in exon 8, suggesting that pathogenic mutations in this exon are related to the optic neuropathy phenotype. Of the dominant *WFS1* variants, c.2051C>T (p.Ala684Val) was found in 6 families reflecting its reported enrichment in the European population, whereas c.2390A>T (p.Asp797Val), c.968A>G (p.His323Arg), and the novel c.2161A>T (p.Asn721Tyr) were identified for the first time in AD disease.[6,40,41]

The novel c.2161A>T (p.Asn721Tyr) variant is predicted to be pathogenic affecting a conserved amino acid. It was also shown to segregate together with optic neuropathy in family D9. All patients with dominant disease in our cohort had early-onset or congenital hearing loss and optic neuropathy with other organ involvement being rare. The exception was the de novo c.937C>T (p.His313Tyr) variant, which has been associated with an early-onset and severe phenotype marked by infantile type 1 diabetes mellitus and congenital hearing loss, as observed for patient P19 in the current study.[40,42,43]

We identified 3 novel recessive *WFS1* variants. The homozygous c.2643_2644delC (p.Phe883Leufs*56) variant was associated with severe syndromic disease. Classification of the c.1372G>A (p.Ala458Thr) variant of patient P27 varies from disease causing to unknown significance depending on the reference database (Table 2). However, a number of adjacent loci (456, 457, and 461) carry previously reported pathogenic variants, which have been associated with Wolfram syndrome, but also with isolated type 1 diabetes mellitus (Human Gene Mutation Database, http://www.hgmd.cf.ac.uk). Patient P27 had optic neuropathy and type 1 diabetes mellitus.

The novel c.2213C>A (p.Ala738Asp) variant is located in a domain with several reported disease-causing variants affecting amino acids 736 to 742. However, the c.2213C>A (p.Ala738Asp) variant is predicted to be benign. The 2 siblings harboring this variant were diagnosed with isolated optic neuropathy at the age of 10 years. One of them (P23) developed polyuria at the age of 30 years, whereas the other (P22) was still without any other organ involvement at the age of 32 years. Although suggestive, the causative role of the c.2213C>A (p.Ala738Asp) variant requires further investigation. Isolated optic neuropathy can be the initial presentation of AR *WFS1* phenotype with other disease manifestations developing much later in life.[44,45]

In addition to the 3 novel variants, the c.1597C>T (p.Pro533Ser) variant was also identified for the first time in patients with optic neuropathy and Wolfram-like syndrome (P24, P25, and P29).[40,46-48] Our data suggest it is disease causing and likely not benign. The c.2648_2651delTCTT 4-bp deletion, which is enriched in Anglo-Saxon populations, was the most frequently identified variant in our families with AR disease (families R3-5 and R9).

This study combined various ophthalmologic data sets of an ultrarare inherited optic neuropathy. Despite some limited data, which is a weakness of the current study, the following features can be considered typical of WON. Both recessive and dominant *WFS1* variants cause progressive optic neuropathy characterized by prominent loss of macular RGCs and accelerated visual deterioration with increasing age. Recessive *WFS1* variants generally cause more severe macular RGC loss and a worse visual prognosis compared with dominant *WFS1* variants, which was confirmed by the PERG and PhNR measurements. To our knowledge, these visual electrophysiological assessments of WON have not been previously reported in the literature.

Furthermore, this study provides further evidence that abnormal lamination and thickening of the OPL on OCT is pathognomonic of AD WON, and the finding of this distinct abnormality should raise the suspicion of an underlying dominant *WFS1* variant. Additional studies are needed to explore the mechanisms by which recessive and dominant *WFS1* variants influence disease severity and progression, both in terms of RGC loss and the development of multisystem deficits.

Funding/Support: This research was supported by the National Institute for Health Research Rare Diseases Translational Research Collaboration (NIHR RD-TRC), the National Institute for Health Research Biomedical Research Centre at Moorfields Eye Hospital NHS Foundation Trust and UCL Institute of Ophthalmology, and the NIHR Moorfields Clinical Research Facility. The views expressed are those of the author(s) and not necessarily those of the NHS, the NIHR or the Department of Health. Financial Disclosures: Anna Majander receives funding from Suomen Silmätutkimusseura ry:n Apurahasäätiö (Finland). Patrick Yu-Wai-Man is supported by an Advanced Fellowship Award (NIHR301696) from the UK National Institute of Health Research (NIHR) and by a Clinician Scientist Fellowship Award (G1002570) from the Medical Research Council (UK), and also receives funding from Fight for Sight (UK), the Isaac Newton Trust (UK), Moorfields Eye Charity, the Addenbrooke's Charitable Trust, the National Eye Research Centre (UK), the International Foundation for Optic Nerve Disease (IFOND), the UK NIHR as part of the Rare Diseases Translational Research Collaboration, the NIHR Cambridge Biomedical Research Centre (BRC-1215-20014), and the NIHR Biomedical Research Centre based at Moorfields Eye Hospital NHS Foundation Trust and UCL Institute of Ophthalmology. Neringa Jurkute is supported by Moorfields Eye Charity (GR001203), National Eye Research Centre (SAC051), National Institute of Health Research Biomedical Research Centre (NIHR-BRC) at Moorfields Eye Hospital and UCL Institute of Ophthalmology. Patrick F. Chinnery, Anthony T. Moore, and Patrick Yu-Wai-Man receive funding from the UK NIHR as part of the Rare Diseases Translational Research Collaboration. Patrick F. Chinnery is a Wellcome Trust Principal Research Fellow (212219/Z/18/Z) and a UK NIHR Senior Investigator, who receives support from the Medical Research Council Mitochondrial Biology Unit (MC_UU_00015/9), the Medical Research Council (MRC) International Centre for Genomic Medicine in Neuromuscular Disease (MR/S005021/1), the Leverhulme Trust (RPG-2018-408), an MRC research grant (MR/S035699/1), an Alzheimer's Society Project Grant (AS-PG-18b-022) and the NIHR-BRC based at Cambridge University Hospitals NHS Foundation Trust and the University of Cambridge. Gavin Arno is supported by a Fight for Sight (UK) Early Career Investigator award (5045/46), Moorfields Eye Charity (Stephen and Elizabeth Archer in memory of Marion Woods), the NIHR-BRC at Moorfields Eye Hospital and UCL Institute of Ophthalmology and the NIHR-BRC at Great Ormond Street Hospital Institute of Child Health. Michel Michaelides receives funding from Moorfields Eye Charity, the Foundation Fighting Blindness (USA), Retina, UK, and The Wellcome Trust (099173/Z/12/Z). Andrew Stockman is supported by the Biotechnology and Biological Sciences Research Council grant BB/R019487/1. All authors attest that they meet the current ICMJE criteria for authorship. Author Contributions: Research design: A.M., P.Y.-W.-M.; Data acquisition and/or research execution: A.M., N.J., F.B., K.B., C.J., H.B.H., M.M.N., C.M.C., H.J.D., S.K., E.B.W., F.K., Y.T.L., M.S., P.F.C., M.B.G., G.A., A.R.W., A.T.M., M.M., A.S., A.G.R., P.Y.-W.-M.; Data analysis and/or interpretation: A.M., N.J., F.B., K.B., H.B.H., M.M.N., G.A., M.M., A.S., A.G.R., P.Y.-W.-M.; Manuscript preparation: A.M., N.J., F.B., K.B., M.M.N., G.A., M.M., A.S., A.G.R., P.Y.-W.-M.

SUPPLEMENTARY MATERIALS

Supplementary material associated with this article can be found, in the online version, at doi:10.1016/j.ajo.2022.04.003.

REFERENCES

1. Takeda K, Inoue H, Tanizawa Y, et al. WFS1 (Wolfram syndrome1) gene product: predominant subcellular localization to endoplasmic reticulum in cultured cells and neuronal expression in rat brain. *Hum Mol Genet*. 2001;10(5):477–484.
2. Schmidt-Kastner R, Kreczmanski P, Preising M, et al. Expression of the diabetes risk gene Wolframin (WFS1) in the human retina. *Exp Eye Res*. 2009;89(4):568–574.
3. Barrett TG, Bundey SE, Macleod AF. Neurodegeneration and diabetes: UK nationwide study of Wolfram (DIDMOAD) syndrome. *Lancet*. 1995;346(8988):1458–1463.
4. Strom TM, Hortnagel K, Hofmann S, et al. Diabetes insipidus, diabetes mellitus, optic atrophy and deafness (DIDMOAD) caused by mutations in a novel gene (wolframin) coding for a predicted transmembrane protein. *Hum Mol Genet*. 1998;7(13):2021–2028.
5. Eiberg H, Hansen L, Kjer B, et al. Autosomal dominant optic atrophy associated with hearing impairment and impaired glucose regulation caused by a missense mutation in the WFS1 gene. *J Med Genet*. 2006;43(5):435–440.
6. Rendtorff ND, Lodahl M, Boulahbel H, et al. Identification of p.A684V missense mutation in the WFS1 gene as a frequent cause of autosomal dominant optic atrophy and hearing impairment. *Am J Med Genet A*. 2011;155A(6):1298–1313.
7. Khanim F, Kirk J, Latif F, Barrett TG. WFS1/Wolframin mutations, Wolfram syndrome, and associated diseases. *Hum Mutat*. 2001;17(5):357–367.
8. de Heredia ML, Clèries R, Nunes V. Genotypic classification of patients with Wolfram syndrome: insights into the natural history of the disease and correlation with phenotype. *Genet Med*. 2013;15(7):497–506.
9. Hilson JB, Merchant SN, Adams JC, Joseph JT. Wolfram syndrome: a clinicopathologic correlation. *Acta Neuropathol*. 2009;118(3):415–428.
10. Bucca BC, Klingensmith G, Bennett JL. Wolfram Syndrome: a rare optic neuropathy in youth with type 1 diabetes. *Optom Vis Sci*. 2011;88(11):E1383–E1390.
11. Bababeygy SR, Wang MY, Khaderi KR, Sadun AA. Visual improvement with the use of idebenone in the treatment of Wolfram syndrome. *J Neuroophthalmol*. 2012;32(4):386–389.
12. Ross-Cisneros FN, Pan BX, Silva RA, et al. Optic nerve histopathology in a case of Wolfram syndrome: a mitochondrial pattern of axonal loss. *Mitochondrion*. 2013;13(6):841–845.
13. Grenier J, Meunier I, Daien V, et al. WFS1 in optic neuropathies: mutation findings in nonsyndromic optic atrophy and assessment of clinical severity. *Ophthalmology*. 2016;123(9):1989–1998.
14. Majander A, João C, Rider AT, et al. The pattern of retinal ganglion cell loss in OPA1-related autosomal dominant optic atrophy inferred from temporal, spatial, and chromatic sensitivity losses. *Invest Ophthalmol Vis Sci*. 2017;58(1):502–516.
15. Majander A, Robson AG, João C, et al. The pattern of retinal ganglion cell dysfunction in Leber hereditary optic neuropathy. *Mitochondrion*. 2017;36:138–149.
16. Richards S, Aziz N, Bale S, et al. Standards and guidelines for the interpretation of sequence variants: a joint consensus recommendation of the American College of Medical Genetics and Genomics and the Association for Molecular Pathology. *Genet Med*. 2015;17(5):405–424.

17. Majander A, Bitner-Glindzicz M, Chan CM, et al. Lamination of the outer plexiform layer in optic atrophy caused by dominant WFS1 mutations. *Ophthalmology*. 2016;123(7):1624–1626.
18. Odom JV, Bach M, Brigell M, et al. ISCEV standard for clinical visual evoked potentials (2009 update). *Doc Ophthalmol*. 2010;120(7):111–119.
19. Bach M, Brigell MG, Hawlina M, et al. ISCEV standard for clinical pattern electroretinography (PERG): 2012 update. *Doc Ophthalmol*. 2013;126(1):1–7.
20. Lenassi E, Robson AG, Hawlina M, Holder GE. The value of two field PERG in routine clinical electrophysiological practice. *Retina*. 2012;32(3):588–599.
21. McCulloch DL, Marmor MF, Brigell MG, et al. ISCEV Standard for full-field clinical electroretinography (2015 update). *Doc Ophthalmol*. 2015;130(1):1–12.
22. Stockman A, Plummer DJ, Montag ED. Spectrally opponent inputs to the human luminance pathway: slow +M and -L cone inputs revealed by intense long-wavelength adaptation. *J Physiol*. 2005;56(pt 1):61–76.
23. Stockman A, Henning GB, Michaelides M, et al. Cone dystrophy with "supernormal" rod ERG: psychophysical testing shows comparable rod and cone temporal sensitivity losses with no gain in rod function. *Invest Ophthalmol Vis Sci*. 2014;55(2):832–840.
24. Chong J, Xia J. MetaboAnalystR: an R package for flexible and reproducible analysis of metabolomics data. *Bioinformatics*. 2018;34(24):4313–4414.
25. Kessel L, Hamann S, Wegener M, Tong J, Fraser CL. Microcystic macular oedema in optic neuropathy: case series and literature review. *Clin Exp Ophthalmol*. 2018;46(9):1075–1086.
26. Matet A, Savastano MC, Rispoli M, et al. En face optical coherence tomography of foveal microstructure in full-thickness macular hole: a model to study perifoveal Müller cells. *Am J Ophthalmol*. 2015;159(6):1142–1151.
27. Reichenbach A, Bringmann A. New functions of Müller cells. *Glia*. 2013;61(5):651–768.
28. Curcio CA, Messinger JD, Sloan KR, et al. Human chorioretinal layer thicknesses measured in macula-wide, high-resolution histologic sections. *Invest Ophthalmol Vis Sci*. 2011;52(7):3943–3954.
29. Monés J, Biarnés M, Trindade F. Hyporeflective wedge-shaped band in geographic atrophy secondary to age-related macular degeneration: an underreported finding. *Ophthalmology*. 2012;119(7):1412–1419.
30. Bringmann A, Reichenbach A, Wiedemann P. Pathomechanisms of cystoid macular edema. *Ophthalmic Res*. 2004;36(5):241–249.
31. Cillino S, Anastasi M, Lodato G. Incomplete Wolfram syndrome: clinical and electrophysiologic study of two familial cases. *Graefes Arch Clin Exp Ophthalmol*. 1989;227(2):131–135.
32. Scaramuzzi M, Kumar P, Peachey N, Nucci P, Traboulsi EI. Evidence of retinal degeneration in Wolfram syndrome. *Ophthalmic Genet*. 2018;40(1):34–38.
33. Simsek E, Simsek T, Tekgul S, et al. Wolfram (DIDMOAD) syndrome: a multidisciplinary clinical study in nine Turkish patients and review of the literature. *Acta Paediatr*. 2003;92(1):55–61.
34. Langwinska-Wosko E, Broniek-Kowalik K, Szulborski K. A clinical case study of a Wolfram syndrome-affected family: pattern-reversal visual evoked potentials and electroretinography analysis. *Doc Ophthalmol*. 2012;124(2):133–141.
35. Arneth B, Arneth R, Shams M. Metabolomics of type 1 and type 2 diabetes. *Int J Mol Sci*. 2019;20(10):2467.
36. Porosk R, Terasmaa A, Mahlapuu R, Soomets U, Kilk K. Metabolomics of the Wolfram syndrome 1 gene (Wfs1) deficient mice. *OMICS*. 2017;21(12):721–732.
37. Farmer K, Smith CA, Hayley S, Smith J. Major alterations of phosphatidylcholine and lysophosphotidylcholine lipids in the substantia nigra using an early stage model of Parkinson's disease. *J Mol Sci*. 2015;16(8):18865–18877.
38. Zmyslowska A, Ciborowski M, Borowiec M, et al. Serum metabolic fingerprinting identified putatively annotated sphinganine isomer as a biomarker of Wolfram Syndrome. *J Proteome Res*. 2017;16(11):4000–4008.
39. Xu H, Valenzuela N, Fai S, Figeys D, Bennett SA. Targeted lipidomics – advances in profiling lysophosphocholine and platelet activating factor second messenger. *FEBS J*. 2013;280(22):5652–5667.
40. Rohayem J, Ehlers C, Wiedemann B, et al. Diabetes and neurodegeneration in Wolfram syndrome: a multicenter study of phenotype and genotype. *Diabetes Care*. 2011;34(7):1503–1510.
41. Rigoli L, Lombardo F, Di Bella C. Wolfram syndrome and WFS1 gene. *Clin Genet*. 2011;79(2):103–117.
42. Hansen L, Eiberg H, Barrett T, et al. Mutation analysis of the WFS1 gene in seven Danish Wolfram syndrome families; four new mutations identified. *Eur J Hum Genet*. 2005;13(12):1275–1284.
43. De Franco E, Flanagan SE, Yagi T, et al. Dominant ER stress-inducing WFS1 mutations underlie a genetic syndrome of neonatal/infancy-onset diabetes, congenital sensorineural deafness, and congenital cataracts. *Diabetes*. 2017;66(7):2044–2053.
44. Smith CJ, Crock PA, King BR, Meldrum CJ, Scott RJ. Phenotype-genotype correlations in a series of Wolfram syndrome families. *Diabetes Care*. 2004;27(8):2003–2009.
45. Ustaoglu M, Onder F, Karapapak M, Taslidere H, Guven D. Ophthalmic, systemic, and genetic characteristics of patients with Wolfram syndrome. *Eur J Ophthalmol*. 2020;30(5):1099–1105.
46. Hardy C, Khanim F, Torres R, et al. Clinical and molecular genetic analysis of 19 Wolfram syndrome kindreds demonstrating a wide spectrum of mutations in WFS1. *Am J Hum Genet*. 1999;65(5):1279–1290.
47. Sam W, Qin H, Crawford B, et al. Homozygosity for a 4-bp deletion in a patient with Wolfram syndrome suggesting possible phenotype and genotype correlation. *Clin Genet*. 2001;59:136–138.
48. Giuliano F, Bannwarth S, Monnot S, et al. Wolfram syndrome in French population: characterization of novel mutations and polymorphisms in the WFS1 gene. *Hum Mutat*. 2005;25(1):99–100.
49. Tessa A, Carbone I, Matteoli MC, et al. Identification of novel WFS1 mutations in Italian children with Wolfram syndrome. *Hum Mutat*. 2001;17(4):348–349.

50. Astuti D, Sabir A, Fulton P, et al. Monogenic diabetes syndromes: locus-specific databases for Alström, Wolfram, and thiamine-responsive megaloblastic anemia. *Hum Mutat*. 2017;38(7):764–777.
51. Crawford J, Zielinski MA, Fisher LJ, Sutherland GR, Goldney RD. Is there a relationship between Wolfram syndrome carrier status and suicide? *Am J Med Genet*. 2002;114(3):343–346.
52. Toppings NB, McMillan JM, Au PYB, Suchowersky O, Donovan LE. Wolfram syndrome: a case report and review of clinical manifestations, genetics pathophysiology, and potential therapies. *Case Rep Endocrinol*. 2018;2018:9412676.
53. Gómez-Zaera M, Strom TM, Rodríguez B, et al. Presence of a major WFS1 mutation in Spanish Wolfram syndrome pedigrees. *Mol Genet Metab*. 2001;72(1):72–81.
54. La Morgia C, Maresca A, Amore G, et al. Calcium mishandling in absence of primary mitochondrial dysfunction drives cellular pathology in Wolfram Syndrome. *Sci Rep*. 2020;10(1):4785.
55. Gasparin MR, Crispim F, Paula SL, et al. Identification of novel mutations of the WFS1 gene in Brazilian patients with Wolfram syndrome. *Eur J Endocrinol*. 2009;160(2):309–316.